**SPEKTRA: Jurnal Fisika dan Aplikasinya**
Volume 8, Issue 2, August 2023
Homepage: doi.org/10.21009/SPEKTRA



DOI: doi.org/10.21009/SPEKTRA.082.02

# SYNTHESIZE OF $TiO_2$ NANOPARTICLES BY PLANETARY BALL MILL FOR DYE-SENSITIZED SOLAR CELLS (DSSC) PHOTOELECTRODE APPLICATION

Ai Nurlaela[1,*], Elvan Yuniarti[2], Siti Ahmiatri Saptari[2]

[1]*Prodi Tadris Fisika, Fakultas Ilmu Tarbiyah dan Keguruan, Universitas Islam Negeri Syarif Hidayatullah Jakarta. Jl. Ir. H. Juanda No 95. Ciputat-Tangerang Selatan, Banten 15412, Indonesia*
[2]*Prodi Fisika, Fakultas Sain dan Teknologi, Universitas Islam Negeri Syarif Hidayatullah Jakarta. Jl. Ir. H. Juanda No 95. Ciputat-Tangerang Selatan, Banten 15412, Indonesia*

*Corresponding Author Email: ai.nurlaela@uinjkt.ac.id

**Received**: 30 June 2023
**Revised**: 13 August 2023
**Accepted**: 15 August 2023
**Online**: 25 August 2023
**Published**: 30 August 2023

**SPEKTRA**: Jurnal Fisika dan Aplikasinya
p-ISSN: 2541-3384
e-ISSN: 2541-3392

## ABSTRACT

In this study, the production of $TiO_2$ nanoparticles from microcrystalline powder was accomplished using the high-energy ball milling (HEBM) technique. Three samples were milled for 0.5, 1, and 1.5 hours. The unmilled powder was also characterized as a comparison. The X-ray diffraction (XRD) technique was utilized to investigate the changes in the microstructure of the milled powders over time. The XRD curve of milled samples showed the broadening of the diffraction peaks, which indicates a decrease in particle size after the milling process. Using the Debye–Scherrer relation, obtain the particle size that decreased from 138.43 nm before milled to 76.65 nm after 0.5 hours milled, 90.63 nm after 1 hour milled, and 83.05 nm after 1.5 hours milled. XRD analysis also showed that $TiO_2$ was in an anatase phase before and after milling. Furthermore, two samples of $TiO_2$, unmilled and after 0.5 hours milled, were used as a working photoelectrode of DSSC with dye from mustard leaves. DSSC efficiency was measured with a 1000-watt halogen lamp. The efficiency of DSSC with photoelectrodes using $TiO_2$ after 0.5 hours milled, which is 0.1715, was higher than using $TiO_2$ before milled, which is 0,0987. The Large surface area in $TiO_2$ enhances the efficiency of DSSC, indicating that the HEBM technique is quite suitable for producing these nanoparticles for this aim.

**Keywords**: $TiO_2$, nanoparticles, XRD, UV-Vis, DSSC efficiency

## INTRODUCTION

Titanium dioxide ($TiO_2$) is a well-known semiconductor material with various properties such as non-toxic, high resistance to corrosion, biocompatible, abundant, absorbing UV light, and scattering visible light efficiently[1] Due to these properties, $TiO_2$ has been widely used in numerous applications nowadays as drug delivery for medicine, as a sunscreen component for cosmetics, as ink and pants for food and plastic colorant, and as a semiconductor material for photovoltaic device [1,2]. In this research, we focus on applying $TiO_2$ as a DSSC photoelectrode.

DSSC is one type of solar energy that changes light into electrical energy, as a three-generation cell developed by Prof. Gratzel and Brian O'Regan in 1991 [3,4]. Due to the depletion of fossil fuels, solar energy is one of the most promising future energy resources to overcome the problem of shortage of energy sources [5,6]. DSSC is cheap and more accessible to produce than silicon-based solar cells. The working electrode, sensitizer (dye), electrolyte, and counter electrode are four key variables for a DSSC. The DSSC working principle involves four basic steps: light absorption by a photosensitizer (dye), electron injection into the conduction band of the working electrode, transportation of carrier between the working electrode and counter electrode, and collection of current [6,7]. $TiO_2$ is one of the oxide semiconducting materials commonly used as a working electrode due to the broad energy band gap of 3-3.2 eV [6]. Naturally, $TiO_2$ is present in the anatase, rutile, and brookite phases. Rutile is stable, while anatase and brookite are metastable and readily change to rutile when heated. Among the three crystal structures, anatase and rutile are the most prevalent, so much research has been conducted on anatase and rutile [1,8,9].

The particle size of the semiconductor material as the working electrode affects the performance of the DSSC. The smaller the particle size, the larger the semiconductor surface area coated on the ITO glass [8]. Therefore, the absorbed dye and the excitation electrons increase. High-energy ball milling (HEBM) is one of the mechanical techniques to reduce the size of $TiO_2$ particles. HEBM can make nanocrystalline powders of oxide particles without involving high-temperature treatment, which cannot be made by conventional powder metallurgy methods [10-12]. Because the impact energy is much higher than the traditional ball milling energy, HEBM is more effective and efficient in decreasing the size of particles from conventional ball milling. Due to the advantages of the HEBM, we applied this technique in $TiO_2$ nanoparticle synthesis for use as a working electrode on DSSC. FIGURE 1 shows the motions of the balls and the powder during a milling process. The powder particles are subjected to high energetic impact during the high-energy ball milling process. Due to the opposite rotation directions of the bowl and turn disc, the centrifugal forces are synchronized alternately [13]. Several studies have shown a significant particle size reduction through the HEBM technique [10,14,15].

In this study, we use the HEBM technique to produce $TiO_2$ nanocrystals for application as working electrodes in DSSC. We want to obtain $TiO_2$ particles with optimum size, which can improve DSSC performance. Furthermore, to see the effect of crystal size reduction on the performance of DSSC, we made a DSSC prototype with milled nanocrystalline $TiO_2$, which

has the smallest particle size as a working electrode. Moreover, as a comparison, a prototype was also made with unmilled $TiO_2$ as a working electrode. Whereas, as a photosensitizer (dye), we use mustard leaves extract because the previous research reveals that dye extracted from mustard leaves has good optical properties indicated by its ability to absorb UV light [16,17].

## METHOD

The research methods begin with milling available commercial $TiO_2$ powders (purity 99.9%, Sigma Aldrich) in a vessel using a shaker-type HEBM machine with a Ball to Powder Ratio (BPR) of 10:1 by weight percent. The milling process was done in an ambient atmosphere with 0.5, 1, and 1.5 hours. The milled $TiO_2$ powder is then made into a paste by mixing it with gel solution using a mortar for 30 minutes until it transforms into a paste. Meanwhile, as a natural dye sensitizer, we use mustard leaves extract obtained by blending 5 gr mustard leaves into 40 ml aquades. The section of mustard leaves was added with 100 ml methanol, so the natural dye sensitizer from mustard leaves was obtained, as seen in FIGURE 2.

Furthermore, the electrode and counter electrode were prepared by cutting ITO glass with 2 cm × 2 cm size for each electrode. The side part of ITO glass was attached with scotch tape, while the center part of the glass with 1.5 cm × 1 cm size remains. The center part of ITO was coated with $TiO_2$ paste using the doctor blading method and then heated inside an oven for 15 minutes.

Furthermore, the electrode was soaked in a dye for 24 hours. Meanwhile, for the counter electrode, the center part of the ITO glass was coated with carbon made from a candle flame, where the ITO glass was burned until a black color appeared, as seen in FIGURE 3. In the last step, DSSC was assembled like a sandwich with a structure, as presented in FIGURE 4 (a). Finally, both electrodes were clamped using paper clips on the left and right sides, as shown in FIGURE 4 (b). $TiO_2$ powders were characterized by X-ray diffraction, using an X-ray diffractometer with Co Kα radiation, crystalline size was calculated by the Debye Scherrer equation, the dye was described using UV-Vis spectrophotometer, and a lux meter was used to observe DSSC performance under halogen lighting.

## RESULT AND DISCUSSION

### Microstructure of $TiO_2$

FIGURE 5 shows the XRD pattern of milled $TiO_2$ powder for 0.5, 1, and 1.5 hours using Cobalt as a radiation source. For comparison, the XRD pattern of unmilled $TiO_2$ powder is also shown (black line). All samples exhibited the XRD characteristic for the anatase phase with the peaks observed at the angle (2θ) around 29.5$^o$ corresponding to (101) peak, 43.15$^o$ corresponding to (004) peak, 56.39$^o$ corresponding to (200) peak, and 63.47$^o$ correspond to (211) peak [8]. The anatase phase is more admirable to apply in DSSC than a rutile form due to its higher energy band gap of 3.2 eV, whereas the rutile form has a band gap of about 3 eV [8]. Crystalline size was calculated by the Debye-Scherrer formula (Eq. 1*). D* is the nanoparticles' crystalline size, K represents the Scherrer constant (0.98), λ denotes the wavelength of Cobalt (1.7902 Å), and β denotes the full width at half maximum (FWHM),

which is obtained from the XRD pattern. TABLE 1 showed a different crystalline size of TiO2 before and after milling.

FIGURE 5 clearly shows that the peaks become broader and less intense as the milling time increases. This phenomenon can be attributed to the decrease in particle size. That might be due to the reduction in the particle size. As shown in TABLE 2, crystalline size decreased from 138.43 nm before milled to 76.65 after 0,5 hours milled (red line), 90.63 nm after 1 hour milled (blue line), and 83.05 nm after 1.5 hours milled (green line). The smallest crystalline size was obtained for 0.5-hour milling time. The data obtained corresponds to several results of previous studies that the particle size decreases after experiencing the milling process. Salah et al. reported synthesizing and characterizing ZnO nanoparticles from microcrystalline ZnO powder. The particle size has decreased in size from around 600 to 30 nm by the HEBM technique [10]. Amal et al. reported the synthesis of CuO nanoparticles from Cu powder (2-5 µm) using dry high-energy ball milling. The particle size decreased from around one micrometer to around 110 nm after 16 hours of milling [18]. The synthesis and characterization of copper nanoparticles from Cu powder by wet milling were reported by Yadav et al. As the milling time increased, the particle size decreased from an initial size of 200 nm to a final crystallite size of 21 nm upon 40 h of milling [19].

**The Absorption Wavelength of Mustard Dye**

The absorbance spectrum can be examined with a UV-Vis spectrophotometer on the range of 250-800 nm wavelength for mustard leaves. The peak was obtained at a wavelength of 300 nm with the highest absorbance value is 1.5 a.u. Based on absorption wavelength, mustard leaves dye can absorb more light in the range of UV; these materials have a reasonably wide wavelength so that they can absorb a wide range of light spectrum. The results of the UV-Vis spectrophotometer can be seen in FIGURE 6.

The energy gap of the dye determined using the Tauc plot method as represented in EQUATION 2. Where $h$ is Plancks constant ($6.63 \times 10^{-34}$ J.s), $\alpha$ is absorbance coefficient, $A$ is absorbance, $l$ is the thickness of cuvette used, $K$ is the comparison constant, $c$ is the speed of light ($3 \times 10^{8}$ m/s$^{2}$ ), $\lambda$ is the wavelength, and $E$ g is energy gap [16,17]. The results of the energy gap calculation using the Tauc plot method is 2.6 eV. Dye as a sensitizer must have a smaller energy gap than the semiconductor material so that charge separation will happen on DSSC. When dye absorbs emitted photon energy from the light source, the electrons in the dye will excite from HOMO (Highest Occupied Molecular Orbital) condition to LUMO (Lowest Unoccupied Molecular Orbital), which then electron would be transferred to the conduction band in the semiconductor.

**DSSC Performance**

This study calculated the DSSC efficiency experimentally with EQUATION 3, where $P$ max is the maximum power output obtained from the multiplication result of maximum current output and maximum voltage output. Then $A$ is the area surface of DSSC coated photoelectrode part, and $P$ light is the halogen lamp measured using a lux meter, where 1 lux

value equals 0.0079 W/m$^2$. The obtained results can be seen in TABLE 2. Due to the XRD data and electrical testing obtained, $TiO_2$ milled for 0.5 hours is best to apply as a working photoelectrode of DSSC. DSSC performance is affected by crystalline size because as the crystal size decreases, there is a higher capacity for dye attachment to the semiconductor material. Consequently, it leads to an increased absorption of photons. The lower solar efficiency was found in larger particle sizes of $TiO_2$,because a strong back-scattering light and less dye adsorption. In line with the study reported by Jeng et al. for single layer DSSC, smaller particle size of $TiO_2$ layers have higher solar efficiency than those larger particle size of $TiO_2$ [20]. I Maurya at al. reported the enhancement in efficiency resulting from the reduction of particles size of $TiO_2$ [21].

## Mathematical Equation

$$D = \frac{K\lambda}{\beta cos\theta} \quad (1)$$

$$\frac{(\alpha hc)^2}{\lambda} = K\left(\frac{hc}{\lambda} - E_g\right) \quad (2)$$

$$\eta = \frac{P_{max}}{P_{light} \cdot A} x100 \quad (3)$$

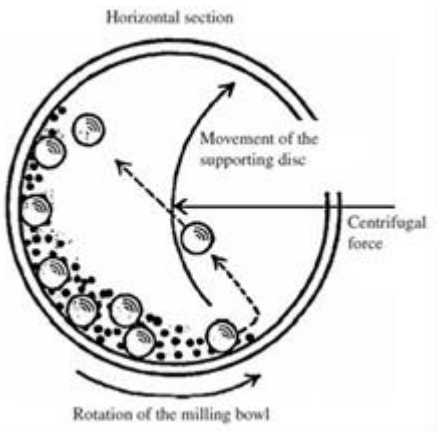


**FIGURE 1.** Schematic view of motion of the ball and powder mixture [6].

**FIGURE 2**. Mustard leaves dye.

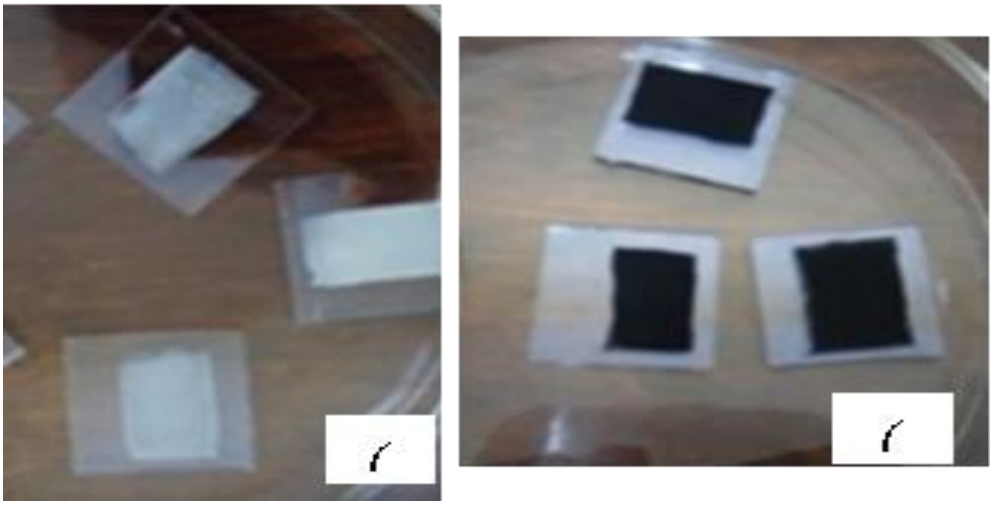

**FIGURE 3**. (a) $TiO_2$ working photoelectrode and (b) counter electrode

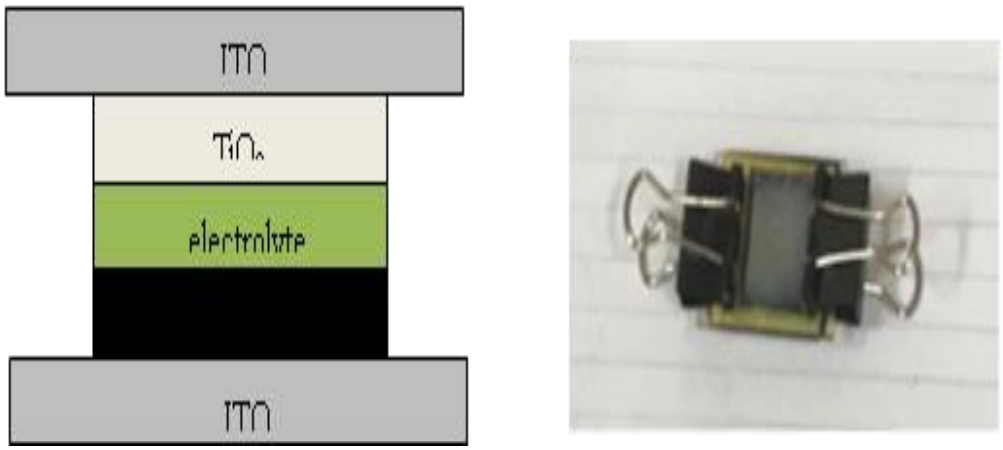


**FIGURE 4**. (a) DSSCs structure and (b) DSSCs prototype

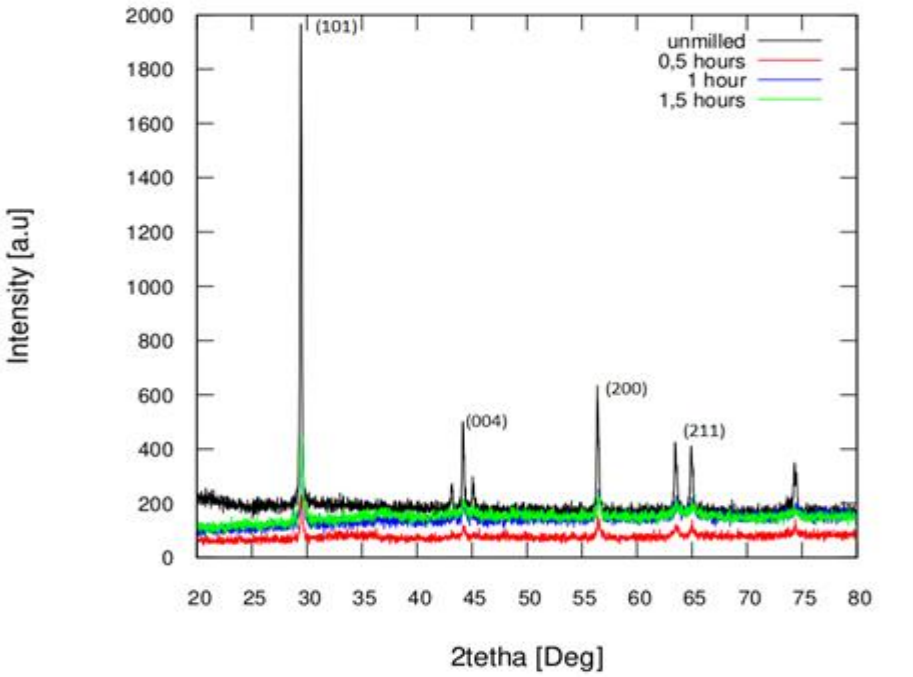


**FIGURE 5**. XRD pattern of unmilled $TiO_2$ and milled $TiO_2$ for 0.5, 1, and 1.5 hours.

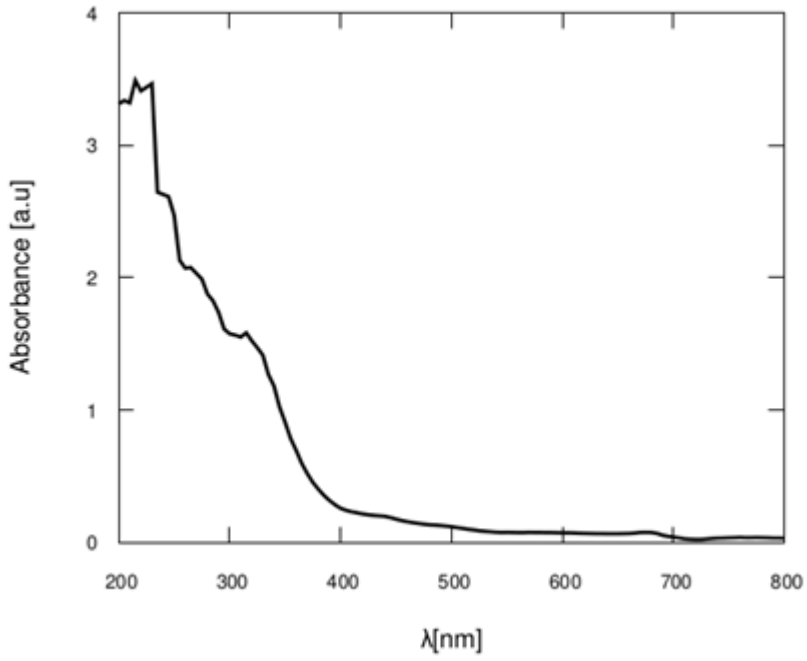


**FIGURE 6**. UV-Vis spectrum from mustard leaves dye.

**TABLE 1.** Crystalline size of unmilled $TiO_2$ and milled $TiO_2$.

| Milling time (hours) | 2θ (°) | FWHM (rad) | Crystalline size (nm) |
|---|---|---|---|
| 0 | 29.43 | 0.001256 | 138.43 |
| 0.5 | 29.51 | 0.130000 | 76.65 |
| 1 | 29.55 | 0.110000 | 90.63 |
| 1.5 | 29.54 | 0.120000 | 83.05 |

**TABLE 2.** DSSCs Performance

| $TiO_2$ | Vm (Volt) | Im (A) | Pm (Watt) | $P_{light}$ (Watt) | η |
|---|---|---|---|---|---|
| Unmilled | 0.001802996 | $2.26983 \times 10^{-6}$ | $4.09250 \times 10^{-9}$ | $4.14276 \times 10^{-6}$ | 0.0988 |
| Milled for 0.5 hours | 0.12024899 | $5.08231 \times 10^{-6}$ | $6.11143 \times 10^{-7}$ | $3.56330 \times 10^{-6}$ | 0.1715 |

## CONCLUSION

This research has succeeded in produced $TiO_2$ nanoparticles by High-energy Ball Milling (HEBM) technique, particle size of $TiO_2$ powder reduce from 138.43 nm before milled to 76.65 nm after 0.5 hours milled. All powder on anatase phase from XRD characterization. The efficiency of DSSCs with photoelectrodes using $TiO_2$ after 0.5 hours milled, which is 0.1715, was higher than using $TiO_2$ before milled, which is 0.0987. The Large surface area in $TiO_2$ enhances the efficiency of DSSCs, indicating that the HEBM technique is quite suitable for producing these nanoparticles for this aim.

## ACKNOWLEDGEMENT

We acknowledge Funding From BOPTN 2020 UIN Syarif Hidayatullah Jakarta. We acknowledge the support of Puslitpen UIN Syarif Hidayatullah Jakarta and PLT UIN Syarif Hidayatullah Jakarta.

## REFERENCES

[1] D. Ziental *et al.*, "Titanium dioxide nanoparticles: Prospects and applications in medicine," *Nanomaterials*, vol. 10, no. 2, p. 387, 2020, doi: 10.3390/nano10020387.

[2] T. Grothe *et al.*, "Photocatalytic properties of $TiO_2$ composite nanofibers electrospun with different polymers," *Norganic Compos. Fibers Prod. Prop. Appl*, pp. 303-319, 2018, doi: 10.1016/B978-0-08-102228-3.00014-1.

[3] S. Aksoy *et al.*, "Li doped ZnO based DSSC: Characterization and preparation of nanopowders and electrical performance of its DSSC," *Physica E: Low-dimensional Systems and Nanostructures*, vol. 121, p. 114127, 2020, doi: 10.1016/j.physe.2020.114127.

[4] C. Pathak *et al.*, "Fabrication and characterization of dye sensitized solar cell using natural dyes," *Materials Today Proceedings*, vol. 12, pp. 665-670, 2019, doi: 10.1016/j.matpr.2019.03.111.

[5] M. Grätzel, "Dye-sensitized solar cells," *Journal of photochemistry and photobiology C: Photochemistry Reviews*, vol. 4, no. 2, pp. 145-153, 2003, doi: 10.1016/S1389-5567(03)00026-1.

[6] K. Sharma, V. Sharma and S. S. Sharma, "Dye-Sensitized Solar Cells: Fundamentals and Current Status," *Nanoscale Research Letters*, vol. 13, pp. 1-46, 2018, doi: 10.1186/s11671-018-2760-6.

[7] C. Ge *et al*., "Graphene-incorporated Photoelectrodes for Dye-sensitized Solar Cells," *Bulletin of the Korean Chemical Society*, vol. 36, no. 3, pp. 762-771, 2015, doi: 10.1002/bkcs.10140.

[8] N. S. Allen *et al*., "The effect of crystalline phase (anatase, brookite and rutile) and size on the photocatalytic activity of calcined polymorphic titanium dioxide (TiO2)," *Polymer degradation and stability*, vol. 150, pp. 31-36, 2018, doi: 10.1016/j.polymdegradstab.2018.02.008.

[9] F. A. Grant, "Properties of rutile (titanium dioxide)," *Reviews of Modern Physics*, vol. 31, no. 3, pp. 646-674, 1959, doi: 10.1103/RevModPhys.31.646.

[10] N. Salah *et al*., "High-energy ball milling technique for ZnO nanoparticles as antibacterial material," *International journal of nanomedicine*, vol. 6, pp. 863-869, 2011, doi: 10.2147/ijn.s18267.

[11] J. Rios *et al*., "Effect of ball size on the microstructure and morphology of mg powders processed by high-energy ball milling," *Metals (Basel)*, vol. 11, no. 10, p. 1621, 2021, doi: 10.3390/met11101621.

[12] C. Dhand *et al*., "Methods and strategies for the synthesis of diverse nanoparticles and their applications: A comprehensive overview," *RSC Advances*, vol. 5, no. 127, pp. 105003-105037, 2015, doi: 10.1039/c5ra19388e.

[13] I. Cao, "Synthesis of Nanomaterials by High Energy Ball Milling," *Skyspring Nanomaterials*, 2018, [Online], Available: https://www.understandingnano.com/nanomaterial-synthesis-ball-milling.html.

[14] A. V. Rane *et al*., "Methods for synthesis of nanoparticles and fabrication of nanocomposites," *synthesis of inorganic nanomaterials*, Woodhead Publishing, pp. 121-139, 2018, doi: 10.1016/B978-0-08-101975-7.00005-1.

[15] A. Vinesh *et al*., "Magnetic anisotropy induced by high energy ball milling of Fe2 MnAl," *Journal of Applied Physics*, vol. 105, no. 7, pp. 14-17, 2009, doi: 10.1063/1.3063676.

[16] M. F. Maulana *et al*., "Dye Sensitized Solar Cell (DSSC) Efficiency Derived from Natural Source," *Jurnal Fisika dan Aplikasinya*, vol. 17, no. 3, p. 68-73, 2021, doi: 10.12962/j24604682.v17i3.9616.

[17] M. Y. Z. A. Nurlaela, E. yuniarti, "Synthesis and analysis of Carbon Dots (CDs) from natural sources," *in Empowering Science and Mathematics for Global Competitiveness*, p. 48, 2019.

[18] M. I. Amal *et al*., "Antibacterial activity of copper oxide nanoparticles prepared by mechanical milling," *IOP Conference Series: Materials Science and Engineering*, vol. 578, no. 1, p. 012039, 2019, doi: 10.1088/1757-899X/578/1/012039.

[19] C. Li *et al*., "Present and future thermoelectric materials toward wearable energy harvesting," *Applied Materials Today*, vol. 15, pp. 543-557, 2019, doi: 10.1016/j.apmt.2019.04.007.

[20] M. J. Jeng *et al*., "Particle size effects of TiO2 layers on the solar efficiency of dye-sensitized solar cells," *International Journal of Photoenergy*, 2013, doi: 10.1155/2013/563897.

[21] I. C. Maurya *et al*., "Effect of Particle Size on the Performance of TiO2 Based Dye-Sensitized Solar Cells," *Chemistry Select*, vol. 3, no. 34, pp. 9872-9880, 2018, doi: 10.1002/slct.201801745.